New Needle-crystalline CR Detector

Paul, J.R. Leblans*, Luc Struye, Peter Willems
Agfa-Gevaert N.V., Research&Development of Materials, Technical Imaging

ABSTRACT

The storage phosphor RbBr:Tl^+ can be grown in needles via vacuum deposition. Thanks to reduced lateral light diffusion thick needle screens still offer acceptable resolution. Due to its low intrinsic X-ray absorption, however, a RbBr:Tl^+ needle screen does not lead to a better absorption/resolution compromise than a $BaFBr_{1-x}I_x:Eu^{2+}$ powder screen. CsBr:Eu^{2+} does combine high specific X-ray absorption and the possibility of needle growth. Its blue emission, peaking at 440 nm and near I.R. stimulation band, with maximum at 685 nm, make it well suited for use in CR systems. Sensitivity and sharpness of a 500 μ thick CsBr:Eu^{2+} needle screen were measured in a flying-spot scanner. The number of photostimulated light quanta per absorbed X-ray quantum is higher than for $BaFBr_{1-x}I_x:Eu^{2+}$. At 70 kVp and 0.5 mm Cu filtration, equal sharpness is obtained for 85% vs. 46% X-ray absorption in $BaFBr_{1-x}I_x:Eu^{2+}$ screens. DQE was measured at 2.5 μGy, 70 kVp, and 0.5 mm Cu filtration for a CsBr:Eu^{2+} needle screen in a flying-spot scanner. Up to 3 lp/mm, DQE was 2 times higher than for state-of-the-art CR systems and equal to the DQE claimed for flat panel DR systems, based on a-Si photodiodes combined with a CsI:Tl scintillator layer.

Keywords: computed radiography, storage phosphor, CsBr:Eu^{2+}, image quality

1. INTRODUCTION

Computed radiography (CR) was introduced as a technology for digital radiography ca. 15 years ago[1]. In CR storage phosphors are used that store energy upon X-ray exposure. A plate containing the storage phosphor is exposed in a light-tight cassette and then read out in a flying spot scanner to create the digital image. Today, CR technology is well established. The system is cheap, has good producibility and is robust.
Direct radiography (DR) systems have been developed that convert X-ray signals into electrical signals, either directly as in a-Se based systems or indirectly as in the systems using a scintillator layer in combination with a-Si photodiodes. Although DR is the common name for a number of different technologies, the perception in the market is that DR, in general, will lead to better image quality than CR. To the specialist, it will be clear that the image quality offered by an indirect system largely depends on the phosphor or scintillator part of the detector.
Excellent image quality is claimed for systems that use CsI:Tl scintillator crystals to convert X-rays into light quanta, which then create charges in an a-Si photodiode[2]. Similar systems using Gd_2O_2S:Tb phosphor plates for conversion of X-ray quanta into light lead to an image quality that is very similar to the image quality offered by state-of-the-art CR systems[3]. CR image quality can be upgraded, therefore, by the use of improved storage phosphor plates.

2. STORAGE PHOSPHOR IMAGE PLATES

2.1. Needle image plate vs. powder image plate

Conventional phosphor plates, used in film/screen radiography and the storage phosphor plates in the Agfa, Fuji and Kodak CR systems are powder plates. The active layer consists of microscopic phosphor crystals, held together by a binder.
The CsI:Tl layer in certain DR systems is an array of phosphor needles with a 5 to 10 μ diameter and a 400 to 500 μ length. Its morphology is similar to that of the CsI:Na scintillator layers used in conventional image intensifiers[3].
A needle plate leads to better image quality than a powder plate for two reasons. The needles act as light guides, thereby strongly reducing light spread in the phosphor layer. As a consequence, image sharpness is much higher at equal thickness. Also, no binder is present, which implies a higher phosphor packing density and, thus, a higher X-ray absorption.

* leblans@twi.agfa.be; phone 03-444-2880; fax 03-444-7655; Agfa-Gevaert N.V., RDM-TI, Septestraat 27, B-2640 Mortsel, België

2.2. CsBr:Eu^{2+} needle imaging plate (NIP)

Today, the storage phosphors $BaFBr_{1-x}I_x:Eu^{2+}$ and $RbBr:Tl^+$ are used in commercial CR systems.
$BaFBr_{1-x}I_x:Eu^{2+}$ is used in the plates of Agfa, Fuji and Kodak and now also Konica. It is an excellent storage phosphor with a high storage capacity[5] and a relatively high specific X-ray absorption. Due to its rather complex chemical composition, $BaFBr_{1-x}I_x$ tends to decompose upon vapor deposition, which makes it impossible to grow a needle-crystalline layer of this phosphor.
$RbBr:Tl^+$ is used in the chest-stands of Konica. Its simple chemical composition allows thermal vapor deposition[6]. Its specific X-ray absorption, for medical X-ray spectra, is, however, much lower than that of $BaFBr_{1-x}I_x$. As a consequence, $RbBr:Tl^+$ needle screens do not lead to better image quality than $BaFBr_{1-x}I_x:Eu^{2+}$ powder screens.
Agfa, in co-operation with SYMYX, discovered an excellent new storage phosphor: $CsBr:Eu^{2+}$.
Its chemical composition and density of 4.5 g/cm^3 lead to a specific X-ray absorption that is similar to that of $BaFBr_{1-x}I_x$.
The relevant spectroscopic and storage phosphor properties of $CsBr:Eu^{2+}$ have been measured.
Image quality of a CR system with the $CsBr:Eu^{2+}$ NIP has been determined and comparison has been made to the image quality of a state-of-the-art CR system and with the image quality of a CsI:Tl based DR system.

3. EXPERIMENTAL

3.1. CsBr:Eu^{2+} NIP preparation

A 500 μ thick $CsBr:Eu^{2+}$ NIP was made via thermal vapor deposition. To this aim, CsBr was mixed with EuOBr and placed in a container in the vacuum deposition chamber. The phosphor was deposited on a glass plate of 25 x 25 cm^2. During vapor deposition, the substrate was rotated at 12 rpm to obtain good thickness homogeneity. A small reference plate was prepared under similar conditions for measurement of the spectroscopic properties and of the conversion efficiency.

3.2 Scanning system for NIP read-out

Read-out was done in a flying spot scanner. The scanning light source was a 30 mW diode laser emitting at 680 nm. A 4 mm Hoya BG-39 (trade name) filter was used to separate the stimulation light from the light emitted by the phosphor screen. Reference $BaFBr:Eu^{2+}$ plates were scanned on the same scanner for sharpness measurement and for measurement of read-out depth.
Pixel size was 100 μ for measurement of the modulation transfer function and for measurement of DQE. For measurement of erasability and read-out depth the pixel size was 50 μ.

3.3. Emission spectrum measurement

Photoluminescence measurements were performed at room temperature on a SPEX DM3000F spectrofluorometer equipped with 0.22 m SPEX 1680 monochromators (resolution 0.1 nm) and a 450 W xenon lamp. The excitation UV-light had a wavelength of 370 nm. The emission spectra were measured and corrected for the photomultiplier sensitivity and for the spectrum distortion by the monochromator.

3.4. Stimulation spectrum measurement

In the stimulation spectrum measurement the photostimulated emission was measured as a function of stimulation wavelength using the following set-up:
The light of a quartz-iodine tungsten lamp was fed into a monochromator and then mechanically chopped with a rotating wheel with a single slit. The second harmonic of the monochromator was eliminated by placing a 4 mm Schott GG435 filter in front of the phosphor screen. By chopping the stimulating light (duty cycle 1/200) only a small fraction of the absorbed energy in the phosphor was released as emission light. The emission light intensity was measured using a photomultiplier tube. Only the AC signal was measured to eliminate the offset caused due to e.g. the dark current of the photomultiplier. A good signal to noise ratio was obtained by averaging several pulses. Correction was made for the wavelength dependence of the tungsten lamp emission intensity and for the transmission of the grating as a function of wavelength.

3.5. Conversion efficiency measurement

The conversion efficiency (C.E.), i.e. the total photostimulated light energy emitted after X-ray exposure was determined for the $CsBr:Eu^{2+}$ NIP and for a screen containing commercial $BaFBr:Eu^{2+}$ storage phosphor.
Prior to X-ray exposure any residual energy still present in the phosphor screen was removed by exposure to light of a 500 W quartz-halogen lamp. The phosphor screen was then exposed with an X-ray source operating at 80 kVp and 5 mA. A 21-mm thick external Al filter was used to harden the X-ray spectrum.
In the measuring set-up a 5-mW diode laser emitting at 690 nm was used to photostimulate the X-ray irradiated NIP phosphor screen and a 10-mW He-Ne laser for the $BaFBr:Eu^{2+}$ plate.
The laser-optics comprised an electronic shutter, a beam-expander and a filter. Using a diaphragm placed in contact with the screen the light emitted by only 7 mm^2 was collected.
The stimulating laser light, transmitted by the screen and the stimulated emission light were separated by a 4 mm BG 39 SCHOTT (trade name) filter in the case of the $CsBr:Eu^{2+}$ NIP and by a 4 mm BG3 SCHOTT (trade name) filter in the case of the $BaFBr:Eu^{2+}$ screen, so that only the emitted light reached the photomultiplier. The signal intensity was measured as a function of time.

3.6. Erasability measurement

The erasability of the $CsBr:Eu^{2+}$ NIP was measured in comparison to a commercial MD-30 (trade name) BaFBr:Eu plate of Agfa-Gevaert N.V.
In a first measurement, both phosphor plates were uniformly exposed to 50 mR at 80 kVp and the scan-average levels (SAL) were determined in the scanner.
In a second measurement, the plates were exposed to much higher doses and then erased with a 500 W (electrical power) quartz-halogen lamp for 1 s. The light intensity at the screen position was measured using a photometer and was 12 mW/cm^2. Higher doses were selected in order to enable signal detection even after erasure without having to adapt the sensitivity settings of the photomultiplier in the scanner. In the second measurement the $BaFBr:Eu^{2+}$ plate was exposed to 44 R and the $CsBr:Eu^{2+}$ NIP to 166 R.

3.7. Measurement of required read-out power

The light energy needed to set free the stored energy upon scanning the $CsBr:Eu^{2+}$ NIP was compared with the light energy needed to scan a $BaFBr:Eu^{2+}$ phosphor plate.
A filter was placed between the stimulating laser and the plate to reduce the laser power on the plate surface to 2 mW.
The screens were scanned a number of times without intermediate erasure until the signal was immeasurably small. From the signal evolution with the number of read-out cycles the read-out depth as a function of read-out energy was calculated. The total photostimulable signal was calculated as the sum of all signals. The read-out depth corresponding to a specific read-out cycle was calculated as the sum of the signals up to that read-out cycle, divided by the total photostimulable signal. The stimulation energy per unit area, SE, corresponding to a certain read-out cycle was calculated as:

$$SE = n \times P \times t / A \qquad (1),$$

where n is the serial number of the read-out cycle, P is the laser power on the plate, t is the scanning time and A is the plate surface.

3.8. DQE measurement

The detective quantum efficiency (DQE) was determined for the $CsBr:Eu^{2+}$ NIP, scanned in the flying spot scanner.
The $CsBr:Eu^{2+}$ plate was uniformly exposed at 70kVp, with 0.5-mm external Cu filtering. The exposure was 2.5 μGy. The X-ray dose was measured with an ionization chamber. The resulting effective energy of the spectrum was 45 keV and the quantum fluence per unit dose is 250.000 quanta/mm^2/mR.
Sharpness was measured for a commercial MD-30 (trade name) BaFBr:Eu plate of Agfa-Gevaert N.V. and for the 500 μ NIP on the laboratory scanner.
For measuring the modulation transfer function (MTF) a bar pattern was imaged with frequencies between 0.025 and 6 lp/mm.
The images were read out with a pixel size of 100 x 100 μ^2.

4. RESULTS

4.1. Emission spectrum

Figure 1 shows the emission spectrum of CsBr:Eu^{2+}. The blue emission, centered around 440 nm allows efficient detection with both a photomultiplier tube and a CCD.

4.2. Stimulation spectrum

Figure 2 shows the stimulation spectrum of CsBr:Eu^{2+}. The stimulation band, centered around 680 nm allows efficient read-out with cheap and compact diode lasers.

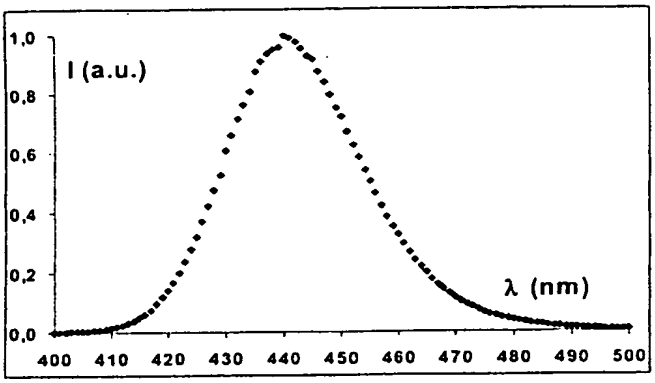

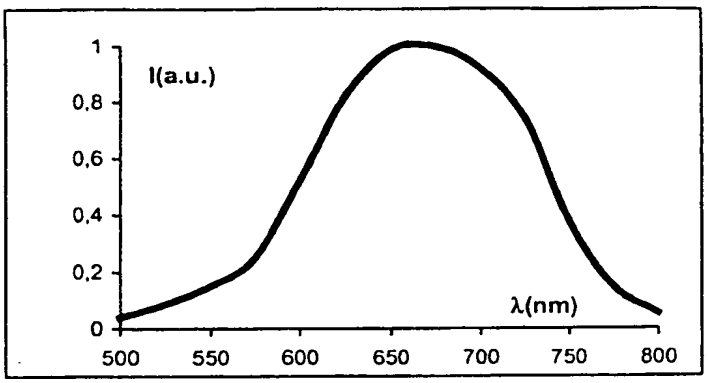

Figures 1 and 2: emission and stimulation spectra of CsBr:Eu^{2+}

4.3. Conversion efficiency

From the intensity curve as a function of time, the total amount of photostimulated light emission energy was calculated. The area under the intensity curve was multiplied by the sensitivity of the system. To this aim, the sensitivity of the photomultiplier and amplifier have been measured as a function of anode-cathode voltage of the photomultiplier and as a function of wavelength. The transmission spectra of the 4-mm BG39 SCHOTT and of the 4-mm BG3 SCHOTT (trade name) filters have been measured.
Because the emission light is scattered in all directions only a fraction of the emitted light is detected by the photomultiplier. The position of the screen with respect to the photomultiplier is such that 10 % of the total emission was detected by the photomultiplier. Correction was made for the limited space angle over which emission was detected. After all these corrections, a conversion efficiency value (C.E.) is obtained in pJ/mm^2/mR. The obtained quantity was divided by the screen thickness to obtain the conversion efficiency per volume of phosphor, i.e. in pJ/mm^3/mR.
Conversion efficiencies of 29 pJ/mm^3/mR for BaFBr:Eu^{2+} and of 37 pJ/mm^3/mR for CsBr:Eu^{2+} were found, respectively. Taking into account the X-ray absorption of the samples, the emission photon energies and the number of X-ray quanta per mR, this corresponds to ca. 500 PSL photons per absorbed 50 keV X-ray quantum for BaFBr:Eu^{2+} and to ca. 750 PSL photons per absorbed 50 keV X-ray quantum for CsBr:Eu^{2+}.

4.4. Erasability

Table 1 lists the SAL results for the first and second measurements.
The erasure depth, i.e. the signal reduction due to exposure to the erasure source, was calculated based on these results and on the doses used in the measurements as:

$$E_d = SAL2 \times dose1 / (SAL1 \times dose2) \qquad (2),$$

and is given in Table 1 for the two phosphors.
It is clear that the CsBr:Eu^{2+} phosphor has a much better erasability than the commercial BaFBr:Eu^{2+} phosphor. Exposure to the same erasure source for the same period of time results in a 100-fold stronger reduction in signal. A much less powerful erasure source can be used, therefore, in a scanner for CsBr:Eu^{2+} NIP's.

Plate → Result ↓	MD-10 BaFBr:Eu^{2+}	CsBr:Eu^{2+}
SAL1 (without erasure)	440	1,180
SAL2 (after erasure)	2,800	290
E_d (erasure signal reduction factor)	7.10^{-3}	7.10^{-5}

Table 1: Measured SAL values and calculated Ed values for MD-10 and CsBr:Eu^{2+} screens

4.4. Read-out depth

Figure 3 shows read-out depth as a function of stimulation energy.

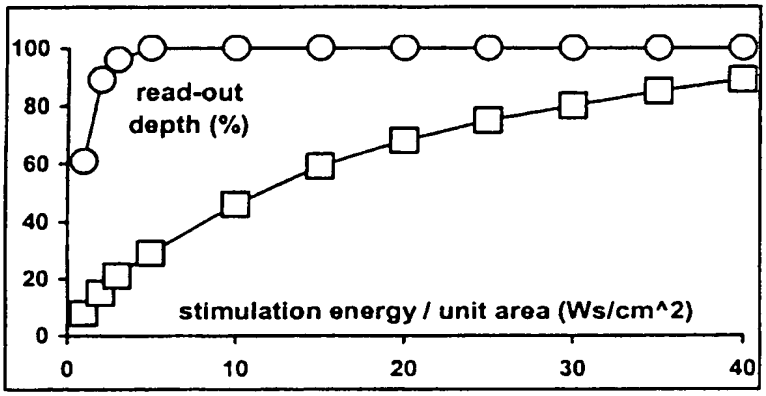

Figure 3: Read-out depth as function of stimulation energy per unit area for CsBr:Eu^{2+} (O) and BaFBr:Eu^{2+} (□)

Much less light energy is needed to set the stored energy free as photostimulated emission in CsBr:Eu^{2+} than in BaFBr:Eu^{2+}. Hence, less powerful light sources can be used in scanners for CsBr:Eu^{2+} and read-out depth can be higher, meaning that a higher gain CR system can be made.

4.5. DQE

The MTF of the system was determined from the square-wave response function (SWRF) of periodic bar patterns. The amplitude response at various spatial frequencies was analyzed between 0.5 and 6 lp/mm. The SWRF was determined by normalizing their amplitudes with respect to the contrast of the bar at the very low frequency of 0.025 lp/mm.
Next, the MTF was calculated from the SWRF according to the relation:

$$MTF(\nu) = \pi/4\ (SWRF(\nu) + 1/3\ SWRF(3\nu) - 1/5\ SWRF(5\nu) + \ldots) \qquad (3).$$

The result, shown in Fig. 4, demonstrates that a 500 μ CsBr:Eu^{2+} NIP leads to a slightly higher sharpness than a 250 μ thick BaFBr:Eu^{2+} powder plate. The absolute MTF values for the MD-30 are lower than those obtained on a commercial CR scanner, meaning that the optics of our laboratory scanner are suboptimal as far as sharpness is concerned.
For the image noise analysis, a uniformly exposed area of 1,024 x 1,024 pixels was used. This region of interest was divided into blocks with a length of 512 pixels and a width of 20 lines. Within each block, the 20 lines are averaged. The noise power spectrum (NPS) per block was calculated for the resulting line with 512 pixels via a 1-dimensional Fourier transformation, and, finally, the NPS blocks were averaged. This procedure was performed with the lines parallel to the fast scan direction and with the lines parallel to the slow scan direction, respectively. Since both NPS were very similar, the DQE was calculated for the NPS in the fast scan direction only.

The DQE was calculated based on MTF and NPS as:

$$DQE(\nu) = MTF(\nu)^2 / (NNPS(\nu) \times n_X) \quad (4),$$

where ν is the spatial frequency, NNPS is the noise power divided by the average signal in mm^{-1} and n_X is the number of quanta per unit area in mm^{-2}.
The DQE of the CR system using the $CsBr:Eu^{2+}$ NIP is plotted as a function of spatial frequency in Fig. 5, together with the DQE of a state-of-the art CR system and the DQE of a DR system based on a-Si photodiodes and a CsI:Tl needle phosphor layer[2].

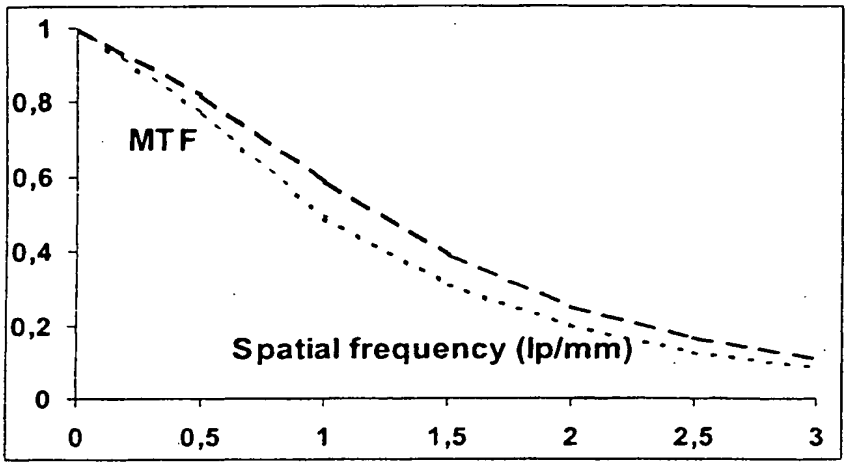

Figure 4: MTF as a function of spatial frequency for a commercial MD-30 phosphor plate, scanned in a commercial scanner (---) and for the 500 m $CsBr:Eu^{2+}$ NIP, scanned in a laboratory scanner (—)

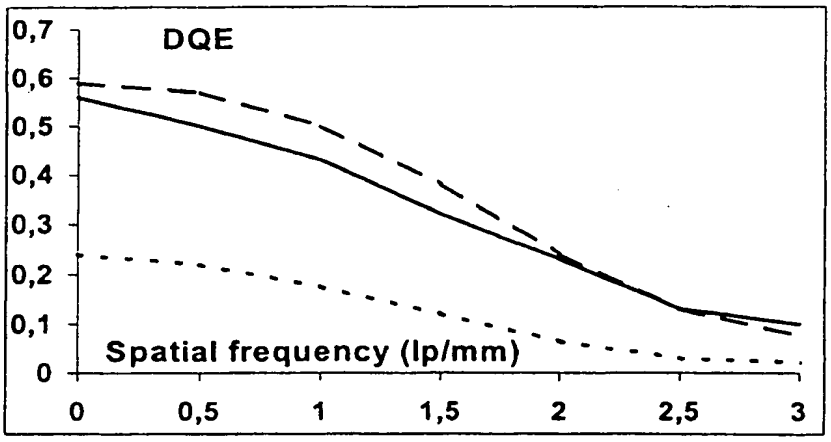

Figure 5: DQE as a function of spatial frequency for state-of-the art CR (---)[8], for the 500 μ $CsBr:Eu^{2+}$ NIP, scanned in a laboratory scanner (—) and for DR with CsI:Tl[2] (—)

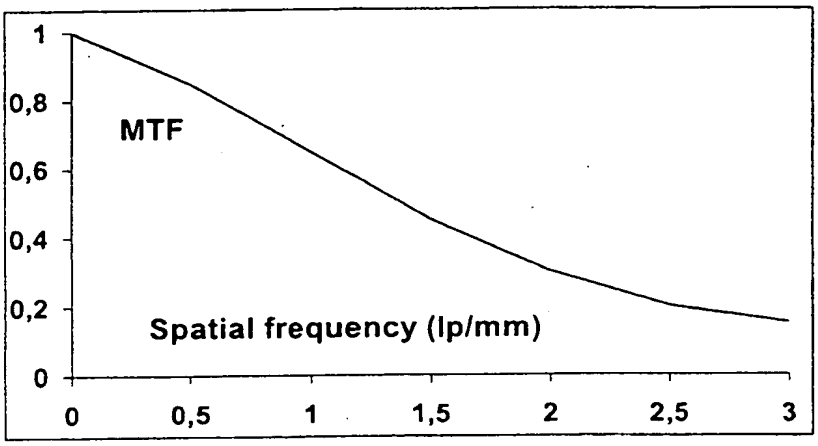

Figure 7: MTF curve that has been used for recalculation of DQE

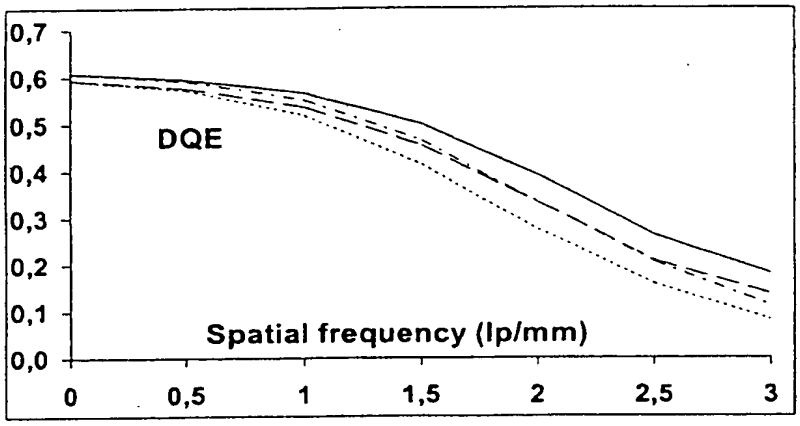

Figure 8: DQE calculated for a CR system with NIP, having a gain of 13 (— – —), having the higher MTF, shown in Fig. 7 (— —) and having both a higher gain and a higher sharpness (——) vs. the DQE of our experimental system (– –)

6. CONCLUSIONS

$CsBr:Eu^{2+}$ is an excellent storage phosphor. It has better phosphor characteristics than $BaFBr_{1-x}I_x:Eu^{2+}$ and it has the advantage that it can be grown in needles.
The emission and stimulation spectra of $CsBr:Eu^{2+}$ are well suited for use in a CR system. $CsBr:Eu^{2+}$ has a higher conversion efficiency and a lower stimulation energy, which makes deeper read-out possible at equal laser power.
CR performance can be improved significantly by using a needle screen instead of a powder screen. A needle screen yields images with acceptable resolution at higher coating weight and, therefore, higher X-ray absorption. A needle screen is less turbid than a powder screen, which leads to lower values for the noise excess factor.
Use of a $CsBr:Eu^{2+}$ needle screen in an exsisting CR system leads to significantly improved image quality. Image quality is equivalent to that offered by the best DR systems. This may offer the possibility to reduce X-ray dose in CR imaging.

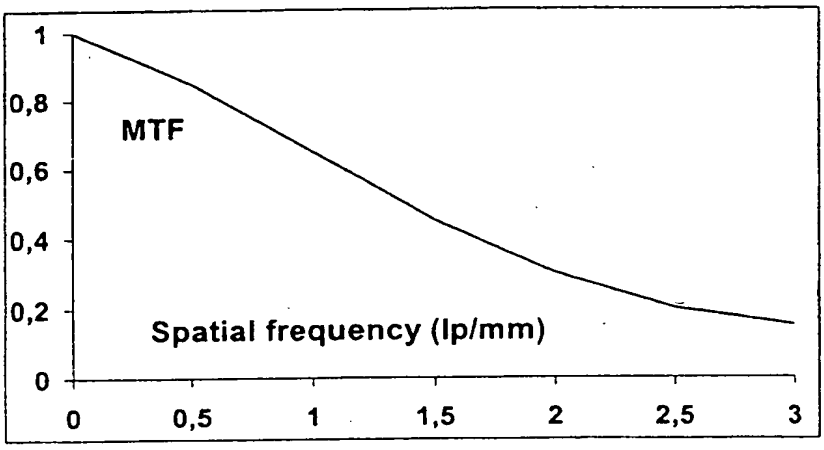

Figure 7: MTF curve that has been used for recalculation of DQE

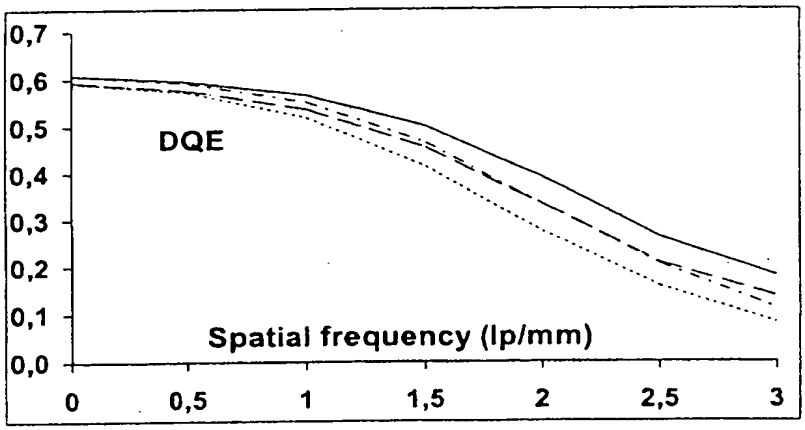

Figure 8: DQE calculated for a CR system with NIP, having a gain of 13 (— – —), having the higher MTF, shown in Fig. 7 (——) and having both a higher gain and a higher sharpness (——) vs. the DQE of our experimental system (– –)

6. CONCLUSIONS

- $CsBr:Eu^{2+}$ is an excellent storage phosphor. It has better phosphor characteristics than $BaFBr_{1-x}I_x:Eu^{2+}$ and it has the advantage that it can be grown in needles.
The emission and stimulation spectra of $CsBr:Eu^{2+}$ are well suited for use in a CR system. $CsBr:Eu^{2+}$ has a higher conversion efficiency and a lower stimulation energy, which makes deeper read-out possible at equal laser power.
CR performance can be improved significantly by using a needle screen instead of a powder screen. A needle screen yields images with acceptable resolution at higher coating weight and, therefore, higher X-ray absorption. A needle screen is less turbid than a powder screen, which leads to lower values for the noise excess factor.
Use of a $CsBr:Eu^{2+}$ needle screen in an exsisting CR system leads to significantly improved image quality. Image quality is equivalent to that offered by the best DR systems. This may offer the possibility to reduce X-ray dose in CR imaging.

AKNOWLEDGEMENTS

We would like to thank Robert Fasbender for measuring the read-out depth and the DQE of the system with NIP.

REFERENCES

1. M. Sonoda, M. Takano, J. Miyahara, H. Kato, "Computed radiography utilizing scanning laser stimulated luminescence", Radiology 148, pp. 833-838, 1983
2. C. Chaussat, J. Chaddal, T. Ducourant, V. Spinnler, G. Vieux, R. Neyret, "New CsI/s-Si 17"x17" x-ray flat-panel detector provides superior detectivity and immediate direct digital output for general radiography systems", *Proc. of SPIE Vol. 3336, Medical Imaging 1998: Physics of Medical Imaging, ed. J.T. Dobbins, J.M. Boone*, pp. 45-56, 1998
3. J.H. Siewerdsen, "Signal, noise, and detective quantum efficiency of a-Si:H flat-panel imagers", *Dissertation submitted in partial fulfillment of the requirements for the degree of Doctor of Philosophy (Physics) in the University of Michigan*, 1998
4. W. Hillen, W. Eckenbach, P. Quadflieg, T. Zaengel, "Signal-to-noise performance in Cesium Iodide X-ray fluorescent screens", *Proc. of SPIE Vol. 1443, Medical Imaging V: Image Physics, ed. R.H. Schneider*, pp. 120-131, 1991
5. M. Thoms, "Photostimulated luminescence: a tool for the determination of optical properties of defect centers", *Journal of Luminescence*, **60-61**, pp. 585-587, 1994
6. M. Nakazawa, O. Morikawa, M. Nitta, H. Tsuchino, F. Shimada, "Effect of protective layer on resolution properties of photostimulable phosphor detector for digital radiographic system", *Proc. of SPIE Vol. 1231, Medical Imaging IV: Image Formation, ed. R.H. Schneider*, pp. 350-363, 1990
7. J.C. Dainty and R. Shaw, *Image Science* (Academic, New York, 1974)
8. J.T. Dobbins III, D.L. Ergun, L. Rutz, D.A. Hinshaw, H. Blume, D.C. Clark, *Med. Phys.* **22 (10)**, p. 1581 (1995)
9. A.R. Lubinsky, B.R. Whiting, J.F. Owen, "Storage phosphor system for computed radiography: optical effects and detective quantum efficiency (DQE), *Proc. of SPIE Vol. 0767, Medical Imaging, ed. S.J. Dwyer, R.H. Schneider*, pp. 167-177, 1987
10. R. Shaw, R.L. Van Metter, "An analysis of the fundamental limitations of screen-film systems for X-ray detection II, Model calculations", *Proc. of SPIE Vol. 0454, Application of Optical Instrumentation in Medicine XII, ed. S.J. Dwyer, R.H. Schneider*, pp. 133-141, 1984